hep-ph/xxxxxxx
FTUV/96-44
IFIC/96-52

Quark mass effects in QCD jets *

G. Rodrigo

Dept. de Física Teòrica, Univ. de València,
E-46100 Burjassot, Valencia, Spain
E-mail: rodrigo@titan.ific.uv.es

Abstract

We present the calculation of the decay width of the Z-boson into three jets including complete quark mass effects to second order in the strong coupling constant. The study is done for different jet clustering algorithms such as EM, JADE, E and DURHAM. Because three-jet observables are very sensitive to the quark mass we consider the possibility of extracting the bottom quark mass from LEP data.

FTUV/96-44
IFIC/96-52
February 1, 2008

*to be published in the Proceedings of the High Energy Physics International Euroconference on Quantum Chromodinamics (*QCD '96*), Montpellier, France, July 1996. Ed. S. Narison, Nucl Phys. B (Proc. Suppl.).

Quark mass effects in QCD jets *

G. Rodrigo [a]

[a]Dept. de Física Teòrica, Univ. de València,
E-46100 Burjassot, Valencia, Spain. E-mail: rodrigo@titan.ific.uv.es

We present the calculation of the decay width of the Z-boson into three jets including complete quark mass effects to second order in the strong coupling constant. The study is done for different jet clustering algorithms such as EM, JADE, E and DURHAM. Because three-jet observables are very sensitive to the quark mass we consider the possibility of extracting the bottom quark mass from LEP data.

1. INTRODUCTION

A precise theoretical framework is needed for the study of the quark mass effects in physical observables because quarks are not free particles. In fact, the quark masses should be seen more like coupling constants than like physical parameters. The perturbative pole mass and the running mass are the two most commonly used quark mass definitions. The perturbative pole mass, $M(p^2 = M^2)$, is defined as the pole of the renormalized quark propagator in a strictly perturbative sense. It is gauge invariant and scheme independent. However, it appears to be ambiguous due to non-perturbative renormalons. The running mass, $\bar{m}(\mu)$, the renormalized mass in the $\overline{MS}$ scheme, does not suffer from this ambiguity. Both quark mass definitions can be related perturbatively through

$$M = \bar{m}(\mu)\left\{1 + \frac{\alpha_{\rm S}(\mu)}{\pi}\left[\frac{4}{3} - \log\frac{\bar{m}^2(\mu)}{\mu^2}\right]\right\}. \quad (1)$$

Heavy quark masses, like the bottom quark mass, can be extracted using QCD Sum Rules or lattice calculations from the quarkonia spectrum, see [1] and references therein. The bottom quark perturbative pole mass appears to be around $M_b = 4.6 - 4.7(GeV)$ whereas the running mass at the running mass scale reads $\bar{m}_b(\bar{m}_b) = (4.33 \pm 0.06)GeV$. Performing the running until the Z-boson mass scale we find $\bar{m}_b(M_Z) = (3.00 \pm 0.12)GeV$. Since for the bottom quark the difference between the perturbative pole mass and the running mass at the M_Z scale is quite significant it is crucial to specify in any theoretical perturbative prediction at M_Z which mass should we use.

The relative uncertainty in the strong coupling constant decreases in the running from low to high energies as the ratio of the strong coupling constants at both scales. On the contrary, if we perform the quark mass running with the extreme mass and strong coupling constant values and take the maximum difference as the propagated error, induced by the strong coupling constant error, the quark mass uncertainty increases following

$$\varepsilon_r(\bar{m}(M_Z)) \simeq \varepsilon_r(\bar{m}(\mu)) \quad (2)$$
$$+\frac{2\gamma_0}{\beta_0}\left(\frac{\alpha_{\rm S}(\mu)}{\alpha_{\rm S}(M_Z)} - 1\right)\varepsilon_r(\alpha_{\rm S}(M_Z)),$$

where $\gamma_0 = 2$ and $\beta_0 = 11 - 2/3N_F$, see figure 1. We use the world average [9] value $\alpha_{\rm S} = 0.118 \pm 0.006$ for the strong coupling constant.

It is interesting to stress, looking at figure 1, that even a big uncertainty in a possible evaluation of the bottom quark mass at the M_Z scale can be competitive with low energy QCD Sum Rules and lattice calculations with smaller errors [2]. Furthermore, non-perturbative contribu-

*Supported by the Conselleria de Cultura, Educaciò i Ciència de la Generalitat Valenciana and CICYT, Spain, under grant AEN-96/1718.

[2]A recent lattice evaluation [10] has enlarged the initial estimated error on the bottom quark mass, $\bar{m}_b(\bar{m}_b) = (4.15 \pm 0.20)GeV$, due to unknown higher orders in the perturbative matching of the HQET to the full theory.

tions are expected to be negligible at the Z-boson mass scale.

The running mass holds another remarkable feature. Total cross sections can exhibit potentially dangerous terms of the type $M^2 \log M^2/s$ that however can be absorbed [3] using Eq. (1) and expressing the total result in terms of the running mass.

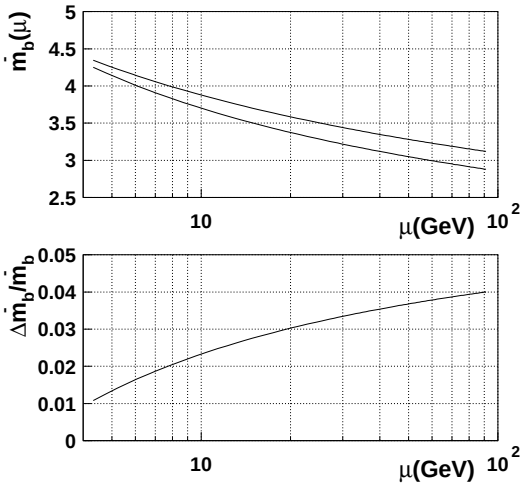

Figure 1. Running of the bottom quark mass from low energies to the M_Z scale. Upper line is the run of $\bar{m}_b(\bar{m}_b) = 4.39(GeV)$ with $\alpha_S(M_Z) = 0.112$. Bottom line is the run of $\bar{m}_b(\bar{m}_b) = 4.27(GeV)$ with $\alpha_S(M_Z) = 0.124$. Second picture is the difference of both, our estimate for the propagated error.

2. THREE JETS OBSERVABLES AT LO

Quark masses can be neglected for many observables at LEP because usually they appear as the ratio m_q^2/M_Z^2. For the heaviest quark produced at LEP, the bottom quark, this means a correction of 3 per mil for a quark mass of 5 (GeV). Even if the coefficient in front is 10 we get at most a 3% effect, 1% if we use the bottom quark running mass at M_Z. This argument is true for total cross section. However, jet cross

Table 1
The jet-clustering algorithms

Algorithm	Resolution
EM	$2(p_i \cdot p_j)/s$
JADE	$2(E_i E_j)(1-\cos\vartheta_{ij})/s$
E	$(p_i + p_j)^2/s$
DURHAM	$2\min(E_i^2, E_j^2)(1-\cos\vartheta_{ij})/s$

sections depend on a new variable, y_c, the jet-resolution parameter that defines the jet multiplicity. This new variable introduces a new scale in the analysis, $E_c = M_Z\sqrt{y_c}$, that for small values of y_c could enhance the effect of the quark mass as $m_b^2/E_c^2 = (m_b^2/M_Z^2)/y_c$. The high precision achieved at LEP makes these effects relevant. In particular, it has been shown [2] that the biggest systematic error in the measurement of $\alpha_S(M_Z)$ from $b\bar{b}$-production at LEP from the ratio of three to two jets comes from the uncertainties in the estimate of the quark mass effects.

We are going to study the effect of the bottom quark mass in the following ratios of three-jet decay rates and angular distributions

$$R_3^{bd} \equiv \frac{\Gamma_{3j}^b(y_c)/\Gamma^b}{\Gamma_{3j}^d(y_c)/\Gamma^d}, \tag{3}$$

$$R_\vartheta^{bd} \equiv \frac{1}{\Gamma^b}\frac{d\Gamma_{3j}^b}{d\vartheta} \Big/ \frac{1}{\Gamma^d}\frac{d\Gamma_{3j}^d}{d\vartheta}, \tag{4}$$

where we consider massless the d-quark and ϑ is the minimum of the angles formed between the gluon jet and the quark and antiquark jets. Both observables are normalized to the total decay rates in order to cancel large weak corrections dependent on the top quark mass [11].

At LO in the strong coupling constant we must compute the amplitudes of the Feynman diagrams depicted in figure 2 plus the interchange of a virtual gluon between the quark and antiquark that only contributes to the two-jet decay rate. In addition to renormalized UV divergences,

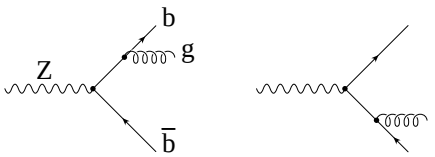

Figure 2. Feynman diagrams contributing to the three-jets decay rate of $Z \to b\bar{b}$ at order $\alpha_{\rm S}$.

IR singularities, either collinear or soft, appear because of the presence of massless particles like gluons. Bloch-Nordsiek and Kinoshita-Lee-Nauemberg theorems[12] assure IR divergences cancel for inclusive cross section. Technically this means, if we use DR to regularize the IR divergences of the loop diagrams we should express the phase space for the tree-level diagrams in arbitrary D-dimensions. The IR singularities cancel when we integrate over the full phase space.

Another delicate question is the problem of hadronization. Perturbative QCD gives results at the level of partons, quarks and gluons, but in nature one observes hadrons, not partons, and hadronization can shift the QCD predictions. We apply to the parton amplitudes the same jet clustering algorithms applied experimentally to the real observed particles, see table 1. Starting from a bunch of particles of momenta p_i we calculate, for instance, $y_{ij} = 2(p_i \cdot p_j)/s$, the scalar product of all the possible momenta pairs. If the minimum is smaller than a fixed y_c we combine the two involved particles in a new pseudoparticle of momentum $p_i + p_j$. The procedure starts again until all the y_{ij} are bigger than y_c. The number of pseudoparticles at the end of the procedure defines the number of jets. The jet clustering algorithms automatically define IR finite quantities. For the moment, we do not enter in the question of which is the best jet clustering algorithm although the main criteria followed to choose one of them should be based in two requirements: minimization of higher order corrections and insensitivity to hadronization. If we restrict to the three-jet decay rate the IR problem can be overcome and everything can be calculated in four dimensions because the jet clustering algorithms automatically exclude the IR region from the three-body phase space.

For massless particles and at the lowest order the EM [7], JADE and E algorithms give the same answers. Analytical results for the massless three-jet fraction exist for both JADE-like [6] and DURHAM [13] algorithms. A complete analysis for the ratios of three-jet decay rates and the angular distributions quoted in Eq. 3 and 4 can be found in [7]. For practical purposes a parametrization of the result in terms of a power series in $\log y_c$ gives a good description [6,7].

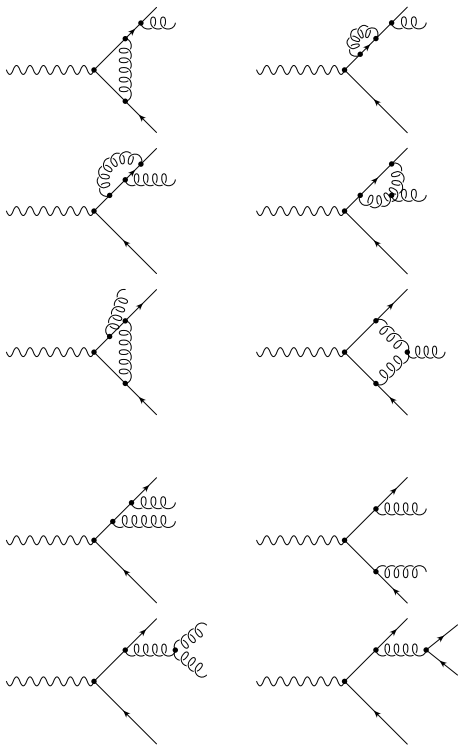

Figure 3. Feynman diagrams contributing to the three-jets decay rate of $Z \to b\bar{b}$ at order $\alpha_{\rm S}^2$. Self-energies in external legs have not been shown.

3. THREE JETS OBSERVABLES AT NLO

The effect of the bottom quark mass has been studied experimentally by [8] on the R_3^{bd} ratio. As we have seen the running of the bottom quark mass from low energies to the M_Z scale is quite strong. The LO QCD prediction for R_3^{bd} does not allow us to distinguish which mass we should use in the theoretical expressions, either the pole mass or the running mass at some scale. The computation of the NLO is mandatory if we want to extract information about the bottom quark mass from LEP data.

At the NLO we have to calculate the interference of the loop diagrams depicted in figure 3 with the lowest order Feynman diagrams of figure 2 plus the square of the tree-level diagrams of figure 3. The amplitudes in the massless case were calculated by [4,5]. The implementation of the jet clustering algorithms was performed by [6].

The main problem that now we can not avoid is the appearance of IR singularities. With massive quarks we loose all the quark-gluon collinear divergences. The amplitudes behave better in the IR region. The disadvantage however is the mass itself. We have to perform quite more complicated loop and phase space integrals. Furthermore, we still conserve the gluon-gluon collinear divergences leading to IR double poles.

The three-jet decay rate can be written as

$$\Gamma_{3j}^b = C[g_V^2 H_V(y_c, r_b) + g_A^2 H_A(y_c, r_b)], \qquad (5)$$

where $r_b = m_b^2/M_Z^2$, $C = M_Z\, g^2/(c_W^2 64\pi)(\alpha_S/\pi)$ is a normalization constant that disappear in the ratio and g_V and g_A are the vector and the axial-vector neutral current quark couplings. At tree-level and for the bottom quark $g_V = -1 + 4s_W^2/3$ and $g_A = 1$. Now we can expand the functions $H_{V(A)}$ in α_S and factorize the leading dependence on the quark mass as follows

$$\begin{aligned} H_{V(A)} &= A^{(0)}(y_c) + r_b B_{V(A)}^{(0)}(y_c, r_b) \qquad (6) \\ &+ \frac{\alpha_S}{\pi}\left(A^{(1)}(y_c) + r_b B_{V(A)}^{(1)}(y_c, r_b)\right), \end{aligned}$$

where we have taken into account that for massless quarks vector and axial contributions are identical[3].

First steep in the calculation is to show the cancellation of the IR divergences in order to build matrix elements free of singularities. It is possible to do it analytically. However, we knew from the beginning IR divergences should disappear [12]. The challenge is in the calculation of the finite parts. This calculation is rather long, complex and full of difficulties. Strong cancellations occur between different groups of diagrams making difficult even a numerical approach. We have taken as guide line the massless result of [4,6] although the IR structure of the massive case is completely different from the massless one.

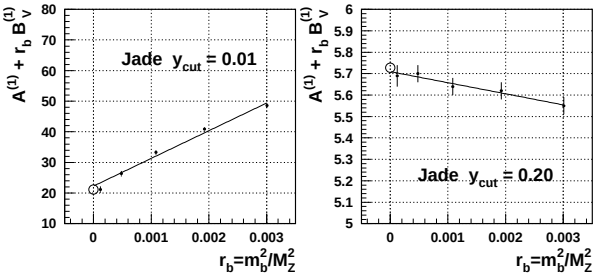

Figure 4. NLO vector contribution to the three-jet decay rate of $Z \to b\bar{b}$ for bottom quark masses from 1 to 5(GeV) and fixed y_c in the JADE algorithm. Big circle is the massless case.

In figures 4 and 5 we present our preliminary result for the vectorial contribution to the $O(\alpha_S^2)$ three-jet decay rate of the Z-boson into bottom quarks. We have performed the calculation for different values of the bottom quark mass from 1 to 5(GeV) for fixed y_c. We want to show we can recover the massless result [6], depicted as a big circle, i.e., in the limit of massless quarks we reach the $A^{(1)}(y_c)$ function. This is our main test to have confidence in our calculation.

In the JADE algorithm we can see that for big values of y_c the NLO corrections due to the quark

[3]We do not consider the small $O(\alpha_S^2)$ triangle anomaly [14]. With our choice of the normalization $A^{(0)}(y_c) = A(y_c)/2$ and $A^{(1)}(y_c) = B(y_c)/4$, where $A(y_c)$ and $B(y_c)$ are defined in [6].

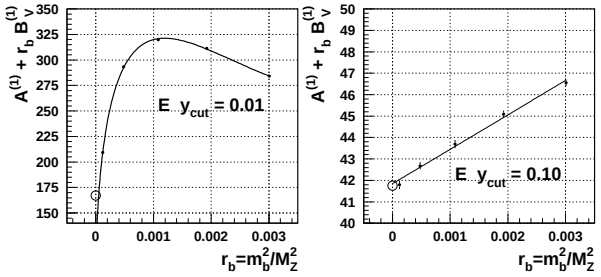

Figure 5. NLO vector contribution to the three-jet decay rate of $Z \to b\bar{b}$ for bottom quark masses from 1 to 5(GeV) and fixed y_c in the E algorithm. Big circle is the massless case.

mass are very small and below the massless result. Notice they increase quite a lot for small values of y_c and give a positive correction that will produce a change in the slope of the LO prediction for R_3^{bd}. In any case we recover the massless limit and a linear parametrization in the quark mass squared could provide a good description.

The E algorithm behaves also linearly in the quark mass squared although only for big values of y_c. Corrections in the E algorithm are always very strong. The reason is the following, the resolution parameter for the E algorithm explicitly incorporates the quark mass, $y_{ij} = (p_i + p_j)/s$, i.e., for the same value of y_c we are closer to the two-jet IR region and the difference from the other algorithms is precisely the quark mass. This phenomenon already manifest at the LO. The behaviour of the E algorithm is completely different from the others for massive quarks. It is difficult to believe in the E algorithm as a good prescription for physical applications since mass corrections as so big. However for the same reason, it seems to be the best one for testing massive calculations.

4. CONCLUSIONS

We have presented the first results for the NLO strong corrections to the three-jet decay rate of the Z-boson into massive quarks. In particular, extrapolating our result we have shown we can recover previous calculations with massless quarks. Their application to LEP data, together with the already known LO, can provide a new way for determining the bottom quark mass and to show for the first time its running.

Acknowledgements. I would like to thank J. Fuster for very encouraging comments during the development of this calculation and for carefully reading this manuscript, A. Santamaria for very useful discussions and S. Narison for the very kind atmosphere created at Montpellier.

REFERENCES

1. G. Rodrigo, hep-ph/9507236.
2. J.A. Valls, Ph.D. thesis, Universitat de València (1994).
3. K.G. Chetyrkin, S.G. Gorishny and F.V. Tkachov, Phys. Lett. B119 (1982) 407. K.G. Chetyrkin, J.H. Kühn and A. Kwiatkowski, hep-ph/9503396.
4. R.K. Ellis, D.A. Ross and A.E. Terrano, Nucl. Phys. B178 (1981) 421.
5. K. Fabricius, G. Kramer, G. Schierholz and I. Schmitt, Zeit. Phys. C11 (1981) 315. G. Kramer and B. Lampe, Fortschr. Phys. 37 (1989) 161.
6. Z. Kunszt and P. Nason, in 'Z Physics at LEP 1', CERN 89-08, vol. 1, p. 373. S. Bethke, Z. Kunszt, D.E. Soper and W.J. Stirling, Nucl. Phys. B370 (1992) 310.
7. M. Bilenky, G. Rodrigo and A. Santamaria, Nucl. Phys. B439 (1995) 505.
8. J. Fuster, these Proceedings.
9. S. Bethke, these Proceedings.
10. G. Martinelli and C.T. Sachrajda, hep-ph/9605336. V. Giménez, G. Martinelli and C.T. Sachrajda, hep-lat/9607018.
11. A.A. Akhundov, D.Y. Bardin and T. Riemann, Nucl. Phys. B276 (1986) 1. J. Bernabéu, A. Pich and A. Santamaria, Phys. Lett. B200 (1988) 569, Nucl. Phys. B363 (1991) 326. W. Beenakker and W. Hollik, Zeit. Phys. C40 (1988) 141.
12. F. Bloch and A. Nordsieck, Phys. Rev. 52 (1937) 54. T. Kinoshita, J. Math. Phys. 3(1962)650. T.D. Lee and M. Nauenberg, Phys. Rev. B133 (1964) 1549.

13. S. Catani et al., Phys. Lett. B269 (1991) 432.
N. Brown and W. Stirling, Zeit. Phys. C53 (1992) 629.
14. K. Hagiwara, T. Kuruma and Y. Yamada, Nucl. Phys. B358 (1991) 80.